Revista Internacional de Investigación e Innovación Tecnológica

Página principal: www.riiit.com.mx

Design and Construction of a Recording Unit for BioMEMS Applications
Diseño y Construcción de una Unidad de Registro para Aplicaciones BioMEMS

Muñoz-Torres, J.A.[a], Martínez-Montejano, R.C.[a]*, Martel-Gallegos, M.G.[a], Chiquito-Cruz, J.A.[b], Muñoz-Torres, T.J.[a]

[a] Facultad de Estudios Profesionales Zona Media de la UASLP. (Orcid: https://orcid.org/0009-0006-9787-3490, https://orcid.org/0000-0002-8996-4134*, https://orcid.org/0000-0002-2048-4896, https://orcid.org/0000-0003-2537-9398).
[b] Facultad de Ingeniería de la UASLP (Orcid: https://orcid.org/0009-0002-4513-0696)
antonio_torres@atrob.group; roberto.montejano@uaslp.mx*; guadalupe.martel@uaslp.mx; jose.chiquito@uaslp.mx; teresita.torres@uaslp.mx

Technological Innovation: Development of a Recording Unit for BioMEMS Applications.
Industrial Application Area: Biotechnological Industry, Recording of Cellular Activity.

Received: June 18, 2025
Accepted: December 18, 2025

Resumen

Los dispositivos conocidos como Sistemas Microelectromecánicos Biológicos (BioMEMS), son diseñados para poder interactuar con muestras biológicas. Un ejemplo que involucra células, es la inyección de reactivos a través de canales manipulados mediante control cartesiano de motores eléctricos para garantizar una dosificación eficiente de la solución. Estas sustancias deben de mantener un nivel apropiado de líquido. El objetivo de este trabajo es el desarrollo e implementación de una Unidad de Registro Celular con las características de que sea viable, en el aspecto económico, de reproductividad y actualización, que permita medir actividad celular *in vitro*. Esta investigación se centra en el diseño combinando eficiencia y calidad considerando la norma ISO 9001:25 y NOM-241-SSA1-2012 para asegurar el cumplimiento de las regulaciones. Se realizaron pruebas que llevaron a una operación de rangos precisos para los sistemas de inyección, micromanipulación y succión, que garantizan funcionalidad y resultados favorables. La unidad de registro celular logra los requerimientos de mantener un continuo y adecuado flujo en los estudios de microperfusión.

Palabras clave: Micromanipulador, Sistema de inyección, Sistema de succión, Unidad de registro celular.

Abstract

Devices known as Biological Microelectromechanical Systems (BioMEMS) are designed to interact with biological samples. An example involving cells is the injection of reagents through channels manipulated by Cartesian control of electric motors to ensure efficient dosing of the solution. These substances must maintain an appropriate liquid level. The objective of this work is the development and implementation of a Cell Recording Unit that is viable in terms of cost, reproducibility, cost-effective upgradability, and user-friendliness, enabling the measurement of in vitro cellular activity. This research focuses on a design that combines efficiency and quality, considering ISO 9001:2015 and NOM-241-SSA1-2012 standards to ensure regulatory compliance. Tests were conducted that resulted in precise operating ranges for the injection, micromanipulation, and suction systems, ensuring functionality and favorable results. The cell recording unit meets the requirements to maintain a continuous and adequate flow during microperfusion studies.

Keywords: Micromanipulator, Injection system, Suction system, Cellular activity recording unit**.**

Introduction

Microelectromechanical systems (MEMS) integrate miniaturized electrical, mechanical, optical, and biological components capable of performing sensing, actuation, processing, and interaction with their environment [1–2]. Within this field, BioMEMS have expanded the development of medical and biological instrumentation, enabling interaction with proteins, cells, reagents, tissues, and other biological media for diagnostic, analytical, or manipulation purposes [3–4].

Micromanipulation—an essential capability in BioMEMS—combines mechanical, electronic, and bioengineering principles to position micropipettes and manage microinjection processes involving very small objects such as cells [5]. A standard injection system includes a micropipette, a positioning mechanism, and pressure-control components that enable precise fluid handling [6–7]. Similarly, flow control is fundamental in microfluidic and micromanipulation applications, often relying on pumping mechanisms that ensure accurate reagent delivery and sample handling [8–9].

Peristaltic-based suction systems, which operate through compression and relaxation of flexible tubing, offer advantages such as chemical compatibility, sterility, and low maintenance [10–11].

Given this context, the present work aims to develop and implement a Cellular Activity Recording Unit that integrates manual and electric micromanipulation, precise reagent injection, and a controlled suction mechanism to enable *in vitro* cellular activity measurements. The scope of this study focuses on the functional design, construction, and evaluation of a low-cost and reproducible prototype compliant with relevant quality standards for the injections of substances into cells. In addition to a suction system with adequate control, which allows measuring cellular activity *in vitro*. The work does not address biological optimization of reagents or long-term cell viability and recording protocols of cellular responses.

The remainder of this article is organized as follows: the methodology describes the mechanical, electronic, and control subsystems that comprise the prototype; the results section presents performance tests for

injection, positioning, and suction; the discussion highlights the system's reproducibility and limitations; and the conclusions summarize the main contributions and potential areas for improvement.

Methodology

The study is exploratory, designed to address a problem from a new perspective and generate a low-cost, accessible prototype of a Cellular Activity Recording Unit for *in vitro* studies in the biochemistry laboratory of the Multidisciplinary Academic Unit Zona Media at UASLP.

The process management was divided into five phases: initiation, involving research and training; planning, with the creation of a work plan and schedule; execution, focused on construction and testing; monitoring and control, to ensure progress; and closure, involving the verification of the prototype's functionality.

A multidisciplinary team and material resources were available, with a total expenditure of $30,148.36 MXN or $1,495.46 USD. Regarding ethical and legal regulations, the development of the instrument applied elements of ISO 9001:2015, particularly in quality planning, operational control, performance evaluation, and continuous improvement. These processes ensured operational integrity, systematic record-keeping, input verification, and periodic performance assessment. The *in vitro* cellular recording unit was classified as a Class II Medical Device due to its role in culture manipulation and analysis. Its development followed NOM-241-SSA1-2012 through design controls, risk management, and manufacturing documentation.

Implementation

Injection System

Firstly, the design of this system was created using Autodesk® Inventor® and AutoCAD® software. Figure 1 shows some of the components designed in these programs, which include: 1 (shelf), 2 (electrovalve holder base), 3 (base cover), 4 (adapter for the female-male harness), 5 (pin for the mechanical locking system), among others.

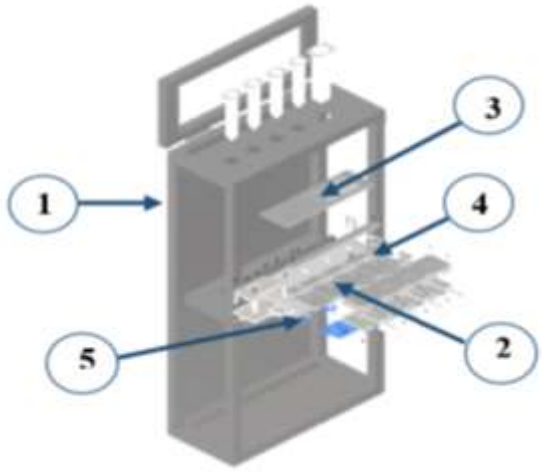


Figure 1. Design of Components for the Injection System.

In the design of the assembled components, a dimensional tolerance of ±0.2 mm was added to the internal walls of the 3D model to ensure proper fitting, resulting in an effective internal clearance of ±0.075 mm when accounting for the expansion of PLA (polylactic acid) used in 3D printing. The injection system components were assembled in Inventor® to ensure proper alignment. The final design, evaluated through simulation, allowed the assembly to be reviewed prior to construction. Additionally, enclosures and four imported Cole-Parmer® solenoid valves were acquired, and their dimensions and specifications were integrated into the final design before fabrication.

The solenoid valves are designed for an approximate lifespan of 2 million cycles, while the integrated silicone or C-Flex tubing is rated for 300,000 cycles, with a response latency of 25 ms. To ensure optimal performance and extend the service life of both components, periodic preventive maintenance typically every 6 to 12 months, depending on operating conditions is essential.

Description of the electronics for the Injection System

The electronics of the injection system allow for precise dosing of liquids in experiments and analyses. Through the electronic controller for the solenoids (Fig. 2) and the user interface, controlled and reproducible injection is achieved, meeting the precision and accuracy requirements necessary in the laboratory environment.

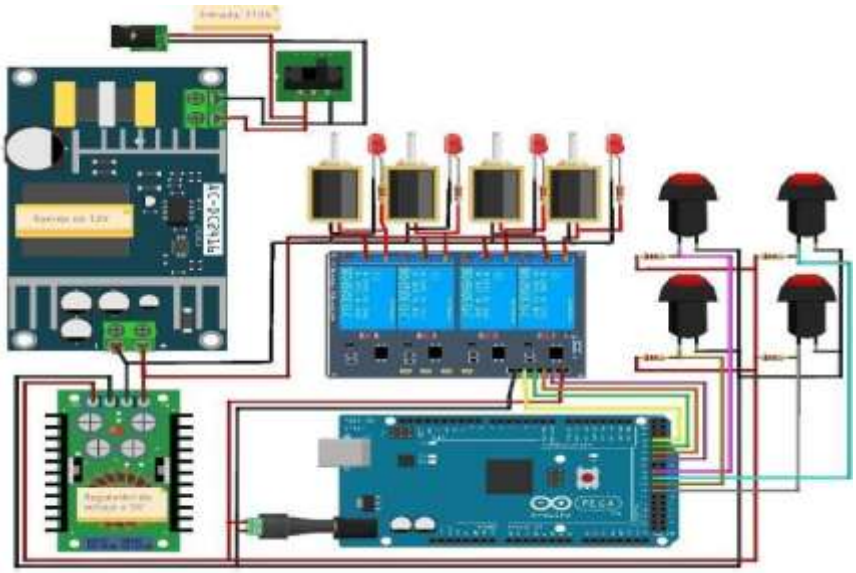


Figure 2. Electronics with Cole-Parmer® 98302-02 Solenoid.

Construction of the Injection System

For the creation of the injection system shelf, type 304 stainless steel was used due to its mechanical properties, ensuring durability. The sections of PTR were cut to form a three-dimensional structure, with bevels at the ends to facilitate welding. The welding, performed with electric arc and E308L electrode, secured the joints, including the cover that protects the syringes. Strips, hinges, and the cover were riveted. Steel sheets were also incorporated on the bottom, back, and top, with holes for the syringes, and a support for the solenoid valves. Finally, the structure was painted to improve its aesthetics and durability.

Injection system programming

The programming process began by defining the input and output variables to connect the Arduino® with the relay module that controls the solenoid valves. Communication, verified through a serial port, was based on the variables configured according to the switches. Additionally, the code is integrated with the micromanipulation system through the shared control module.

Assembly of the Injection System

The assembly of the solenoid valve system begins with the 3D-printed parts, ensuring their fit according to the design. The solenoid is installed in the lower housing, connecting the indicator LED and the solenoid valve

using 2-pin JST connectors to facilitate maintenance. The wiring is routed to a central connector that activates the solenoid. Then, the upper cover secures the valve with 2 mm screws. A locking mechanism allows the housing to slide for maintenance. The solenoids are connected to a 4-relay module controlled by an Arduino® Mega with a 12V power line. Finally, the connections of the solenoid valves, syringes, and hoses to the 3-way valves are verified, ensuring proper flow control to the perfusion chamber.

Operation of the Injection System

To validate the injection system (Fig.3), the operation of the solenoids was verified by activating the switches in the control module. Each solenoid valve must be activated according to its numbering, ensuring that the stem either restricts or allows the flow of liquid when appropriate. The control module integrates functions with the micromanipulation system, using a panel with switches for the four solenoid valves.



Figure 3. Installation of the Injection System.

The signals from the switches are sent to the Arduino® microcontroller, which activates the relays to contract the solenoid stem, improving handling precision. When any switch is pressed, an indicator LED lights up to confirm the activation of the valve, and each solenoid has its own LED to verify its proper functioning.

Micromanipulation System

For the development of the micromanipulation system, Autodesk® Inventor software was used, as shown in Figure 4. It highlights some parts, such as 1 (casings), 2 (adapters), 3 (supports), and 4 (internal parts of the manipulator mechanism). Each part model was adapted to the workspace, in this case, to an inverted fluorescence microscope.

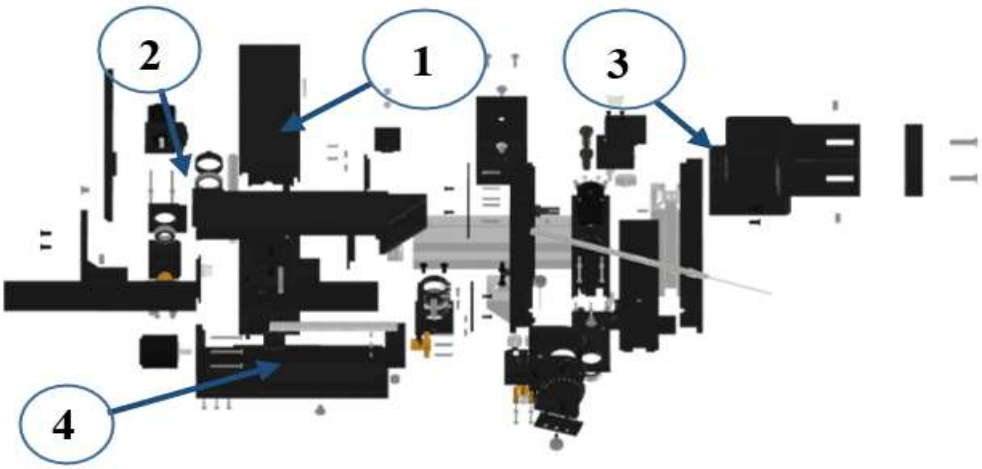


Figure 4. Design parts of the Micromanipulator.

The design of the micromanipulator uses a linear Cartesian kinematics system based on the X, Y, and Z axes to move the links. It includes a pipette holder connected to the injection system, capable of manipulating the angle using gears. The bases of the micromanipulator are designed to attach to the microscope arm, prioritizing stability, precision, and durability. Additionally, it allows for customization of the configuration of the links and the components that make them up.

Analysis of direct kinematics

To carry out the analysis, it is necessary to establish the origin of the coordinate systems of the joints (Fig. 5) [12].

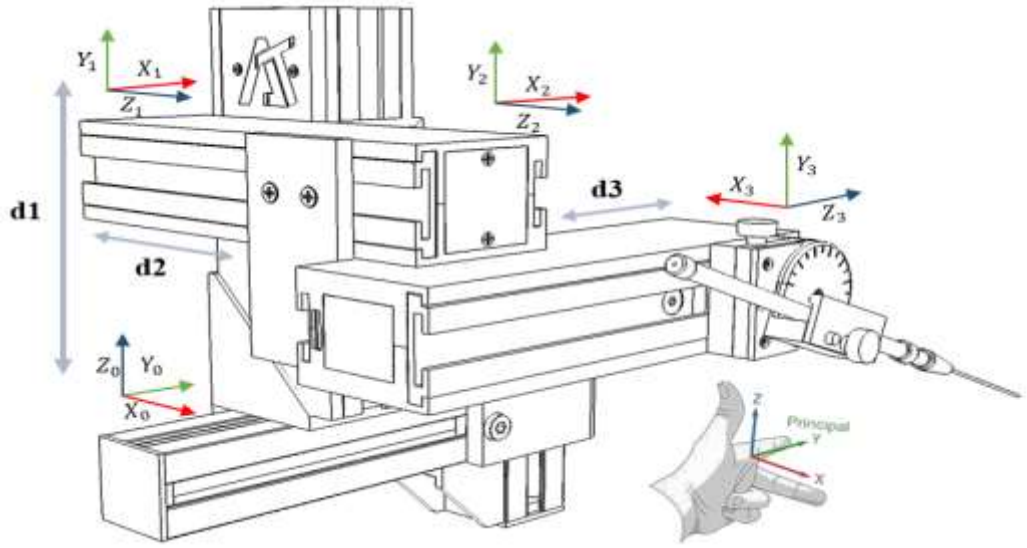


Figure 5. Cartesian robot with 3 degrees of freedom of the micromanipulation system.

The D-H representation (Table 1) of a rigid element depends on 4 geometric parameters associated with each element.

Table 1. Denavit-Hartenberg parameters.

Link	$\boldsymbol{\alpha_i}$	$\boldsymbol{\theta_i}$	$\boldsymbol{d_i}$	$\boldsymbol{a_i}$
1	90°	90°	d1	0°
2	0°	0°	d2	0°
3	-90°	90°	d3	0°

Now, using the following Equation 1, the homogeneous matrices for each link are obtained.

$$A_i^{i-1} = \begin{bmatrix} cos\,cos\,\theta_i & -cos\,cos\,\alpha_i\ sin\,sin\,\theta_i & sin\,sin\,\theta_i & cos\,cos\,\alpha_i \\ cos\,cos\,\theta_i & 0 & sin\,sin\,\alpha_i & 0 \\ 0 & sin\,sin\,\alpha_i & sin\,sin\,\theta_i & a_i \\ cos\,cos\,\theta_i & -sin\,sin\,\alpha_i & cos\,cos\,\theta_i & a_i\,sin\,sin\,\theta_i \\ cos\,cos\,\alpha_i & d_i & 0 & 1 \end{bmatrix} \quad \textbf{(Eq. 1)}$$

From Equation 2, the matrix T (Equation 3) can be calculated, the result of which indicates the system location of the robot with respect to its base.

$$T = A_1^0 A_2^1 A_3^2 \quad \textbf{(Eq. 2)}$$

$$T = [0\ 0\ 1\ 0\ 1\ 0\ 0\ 0\ 0\ 1\ 0\ d_1\ 0\ 0\ 0\ 1\ ] * [1\ 0\ 0\ 0\ 0\ 1\ 0\ 0\ 0\ 0\ 1\ d_2\ 0\ 0\ 0\ 1\ ] * [0\ 0\ -1\ 0\ 1\ 0\ 0\ 0\ 0\ -1\ 0\ d_3\ 0\ 0\ 0\ 1\ ] \quad \textbf{(Eq. 3)}$$

The values of the matrix from Equation 4 are presented, obtained by multiplying the homogeneous matrices from Equation 3, which allows for the calculation of the direct kinematics of a robot.

$$T = [0\ -1\ 0\ -d_1\ 0\ 0\ 1\ 0\ -1\ 0\ 0\ d_3 + d_2\ 0\ 0\ 0\ 1\ ] \quad \textbf{(Eq. 4)}$$

Description of the electronics for the Micromanipulation System

The electronics of the micromanipulation system provide the precise control and feedback necessary to manipulate objects at the microscopic level. That is, through the motion controller, the motors (Fig.6), and the user interface, precise and controlled movements are achieved in the micromanipulation system.

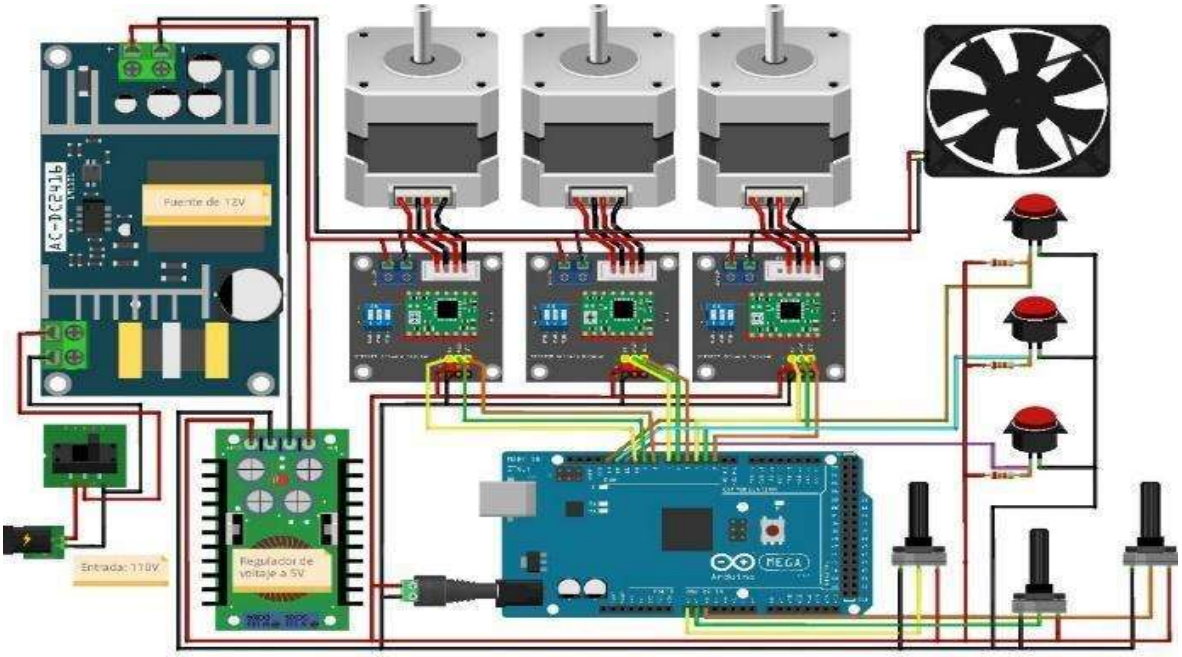


Figure 6. Wiring Diagram of the Micromanipulation System.

Construction of the suction system

The construction of the micromanipulator required detailed planning to ensure functionality and precision. 3D printing with PLA material was used due to its rigidity, strength, and low cost. The system includes approximately 50 printed parts, such as housings, adapters, and supports, which are essential for assembly. All the parts were inspected to ensure quality, precision, and correct assembly of the micromanipulator.

Programming of the Micromanipulation system

The programming process began by defining the input and output variables. The output signals establish communication between Arduino® and the values sent by the potentiometers, which control the sliding of the

micromanipulator's axes via a serial port.

Assembly of the Micromanipulation system

For the assembly of the micromanipulation system, 3D-printed parts and fitted components were used to ensure precision. The assembly began with the installation of the motor adapter to the lead screw, which generates linear motion. The screw was stabilized using a support with a 688ZZ 8x16x5 bearing and a retaining ring. Next, the rail was assembled onto the support, which contains the Acme nut to move the sliding adapter. Finally, the housings were placed to protect the mechanism and prevent undesired movements. The micromanipulator arm was attached to the base, made of Rexroth aluminum profiles 3 c, ensuring stability and precision during use with the microscope.

Operation of the Micromanipulation system

To verify the functionality of the system, the micromanipulator was mounted on the microscope, and the wiring connections for each link were made. The hoses were adjusted to place the pipette in the working area (Fig. 7). The micromanipulator can be manually adjusted by loosening screws, allowing for free initial positioning. For precise movements, linear displacement controlled by motors is used.



Figure 7. Installation of the micromanipulation system.

The control module features rotary knobs that allow the links to move left to right and up and down. These movements, limited to prevent damage, enable centering the micropipette capillary under the microscope, facilitating tests such as liquid replacement and reagent flow.

Control module

To operate the solenoids of the injection system and control the axes of the micromanipulation system, a module was designed in Inventor® that integrates both systems into a single tool, making it easier to use. Although they operate together, each system functions independently. The micromanipulator is controlled via three knobs, one for each axis, and push buttons to calibrate the links. The module's panel includes switches to operate the solenoids of the injection system, as well as a power on/off switch, providing a simple and efficient user interaction.

Suction system

Figure 8 shows the structure of the suction system, including 1 (base), 2 (protective cover for the fan), 3 (support structure for the touchscreen), 4 (screen housing), 5 (protective cover or box for the pump), among others. Also included are components corresponding to 6 (peristaltic pump), such as 7 (housing), 8 (heads), 9 (hose holder), etc.

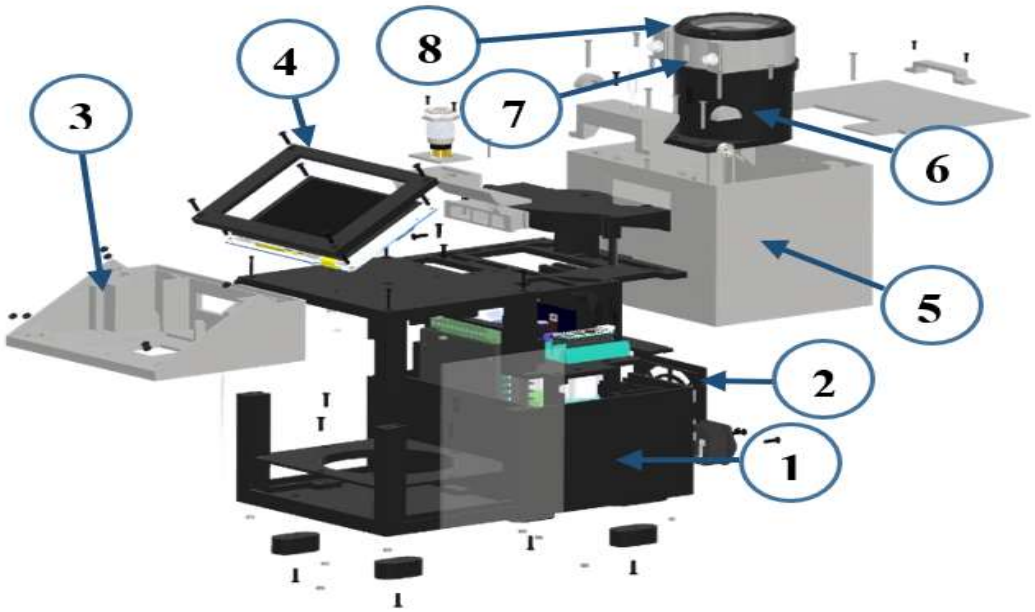


Figure 8. Suction System Design Inventor®-Assembly.

The assemblies of the peristaltic pump and suction system were created in Inventor® to evaluate their design prior to 3D manufacturing. The pump includes a 5-roller head, silicone tubing, adapters, and a protective acrylic cover. The suction system, designed to contain liquids and facilitate transport, incorporates a Nextion® HMI screen, ventilation with protection, and rubber supports for stability. Its final design integrates the structure, pump, electronics, and screen, ensuring functionality, easy maintenance, and aesthetic.

Pump flow rate calculation

The flow rate of a peristaltic pump depends on the tube diameter, the rotor speed, and the number of rollers, thus determining the amount of liquid pumped over a specific period of time. A higher number of rollers produces a more continuous and uniform flow by reducing pulsation; however, it decreases the volume displaced per roller and increases friction and tube wear. In contrast, fewer rollers generate higher pulsation but displace a larger volume per compression event. Tube stiffness is also a determining factor: a stiffer tube requires greater force to achieve full occlusion, and incomplete occlusion leads to fluid backflow, reducing the actual flow rate and increasing the mechanical load on the motor. A more flexible tube improves volumetric efficiency but may deform excessively, reducing its service life. Finally, increasing motor speed raises the theoretical flow rate, but excessively high speeds may reduce actual flow due to material hysteresis and accelerate wear, whereas lower speeds promote elastic recovery of the tube and improve flow accuracy, particularly in microdosing applications.

In this case, five rollers are used to obtain a more continuous and uniform flow (Fig. 9). A silicone tube with a hardness of 60A, considered medium, is employed, providing an adequate balance between flexibility and firmness. This material withstands temperatures ranging from −60 to 275 °F and has an approximate service life of 1,000 hours. Additionally, the system features adjustable speed; for the studies conducted, a

low speed is selected, which helps reduce friction-induced wear from the five rollers and promotes proper elastic recovery of the silicone tube.

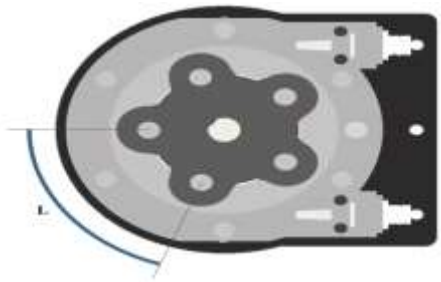


Figure 9. Measurement of length L.

Volume captured between 2 rollers = (cross-sectional area of the hose) * (length of the fluid L), as in Equation 5 [13].

$$V = \left(\frac{\pi}{4D^2}\right) * (L) \qquad \textbf{(Eq. 5)}$$

Since the pump model consists of 5 rollers, the captured volume must be multiplied by 5. With this, the pump displacement is obtained in Equation (6).

$$V_{total} = \left(\frac{\pi}{4D^2}\right) * (L) * 5 \qquad \textbf{(Eq. 6)}$$

Considering the dimensions of the real system, D = 3 cm and L = 36.25 cm, the total volume is 15.81 cm³. The theoretical volumetric flow rate (Q_theoretical) is obtained by multiplying the total volume by the motor speed in RPM; in this case, the RPM is fixed at 75, resulting in Q_theoretical = 1,185.75 cm³/min. The volumetric efficiency of the pump is determined using Equation 7, considering a Q_real value of 1,063 cm³/min. Finally, the percentage error corresponding to the difference between the theoretical and real volumes is 10.3%, as calculated using Equation 8.

$$nV = \frac{Q_{Real}}{Q_{theoretical}} = (1{,}063/1{,}185.75) * 100 = 89.7\% \qquad \textbf{(Eq. 7)}$$

$$Error\ (\%) = \left|\frac{(Q_{Theoretical} - Q_{Real})}{Q_{Theoretical}}\right| x\ 100 = \left|\frac{(1185.75 - 1063)}{1185.75}\right| x\ 100 = 10.3\% \qquad \textbf{(Eq. 8)}$$

Electrical connections of the suction system

The suction system requires a prior analysis of electrical connections to ensure proper operation. Figure 10 shows the connection diagram between components, preventing short circuits and improving efficiency. The microcontroller and voltage regulator are cooled by a fan, and the TB6600 driver operates at 1.5A, ¼ microstep, powered by 24V.

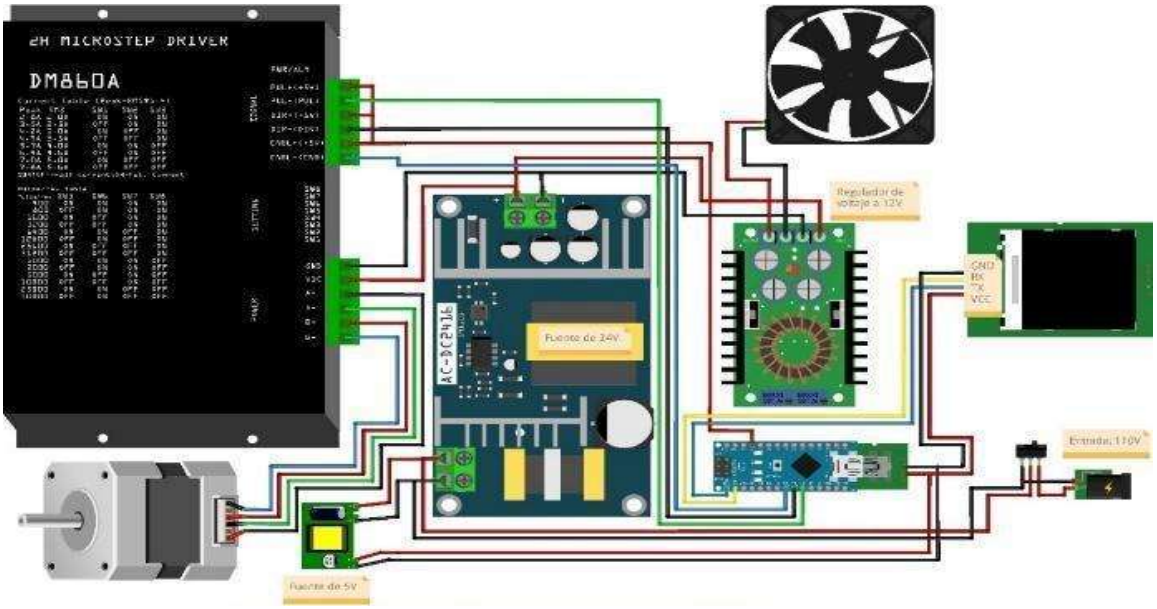


Figure 10. *Connection diagram of the suction system.*

Construction of the suction system

The suction system was built using 3D printing of approximately 60 pieces in PLA, including the structure and the peristaltic pump. The parts were designed to ensure strength and precision in the assembly. During the assembly, adequate space for the electronic components was verified, preventing unwanted contact that could cause short circuits. The installation was carried out with specific tolerances for an optimal fit, using snap nuts to secure the assembled parts and ensure the stability of the system during operation.

Programming of the suction system

The programming process defined input and output variables to connect Arduino® and Nextion® via the serial port, verifying their communication. The Arduino® microcontroller programming was based on the variables configured in the Nextion® interface.

Suction system assembly

The suction system includes electronic control, a peristaltic pump, and an overall structure. For assembly, the pump base was attached to the Nema 23 motor, the wiring was routed through the housing, and the head with 5 rollers and 688ZZ bearings (16x8x5 mm) was mounted. The head was secured to the rotor, and a top cover was installed to protect the silicone tube while allowing internal visibility. The structure includes a fan with a duct and protective cover for cooling, an electrical system connected to the voltage regulator, and a screen shielded with a cover designed to prevent damage. The assembly ensures both functionality and aesthetic appeal of the system.

Testing and verification of the suction system

After construction, programming, and assembly, tests were conducted on the suction system. The Nextion® and Arduino® programs were successfully loaded, enabling proper operation. The system is activated via a switch that directs to the main menu, where the direction, motor activation, and suction speed can be adjusted (Fig. 11). The liquid is sucked by the peristaltic pump and stored for disposal, with the flow controlled using speed adjustment buttons within the screen interface.



Figure 11. Suction system power-on - main menu.

Integration of the cellular activity recording unit

During the development of the Cellular Activity Recording Unit, the necessary modules were integrated into the workspace, considering the arrangement of instruments and their interactions. The unit starts with an injection system that manages reagents and solutions in the perfusion chamber, controlled by a module that activates solenoids to release the reagents into the micropipette on the micromanipulator. Then, the micromanipulation system, coupled to a fluorescence microscope, allows the distribution of reagents and observation of cellular reactions. A suction system maintains the flow and cleanliness of the chamber. All data is stored on a PC for analysis, achieving efficient integration of the devices (Figure 12).



Figure 12. Integration of the Cellular Activity Recording Unit.

The micromanipulation system currently operates manually and functions as an open-loop control system without sensory feedback. However, its design does not limit the possibility of integrating automation in future versions by incorporating motors and position sensors to improve precision and repeatability. This would allow the prototype to evolve into an automated system with feedback (closed-loop control), optimizing its performance and reliability.

The current integration of the prototype allows the entire system to be operated through a single module, enabling a single operator to manage simultaneous tasks. Additionally, this integration facilitates more efficient maintenance, especially when identifying areas for improvement

within the system. Likewise, maintenance and replacement costs remain low due to the affordable components and the ease of reprinting parts, including consumables with predictable wear, such as tubing.

Functionality Preliminary Test of Cellular Activity Recording Unit

To evaluate the functionality of the integrated system, preliminary tests were conducted in the absence of cellular samples. The objective was to regulate the flow rate of the maintenance solution supplied to the perfusion chamber and to synchronize it with the extraction rate of the suction system in order to maintain a constant liquid level and volume. Approximately 40 mL of distilled water were loaded into a 50 mL syringe, the connected tubing was primed, and the flow rate was regulated using the drip controller of a commercial intravenous infusion set. Once the maximum liquid level in the perfusion chamber was reached, the suction system was activated and several operating ranges were evaluated until a stable equilibrium was achieved without volume backflow. Subsequently, the microinjection system was assessed to verify that the injected volume did not significantly alter the established liquid level and that the exchange flow remained constant. For this purpose, 3 mL of a 1% trypan blue solution were loaded into a 20 mL syringe, the line connected to the micropipette was primed, and the capillary tip was positioned at the center of the microscope's field of view under bright-field illumination. Finally, the solenoid valve was actuated to release the solution, and the resulting flow rate and exchange pattern were monitored.

Results

Tests were conducted on the Cellular Activity Recording Unit to ensure the proper functioning of the solution flow and replacement in the perfusion chamber (Fig. 13). Initially, the flow of the maintenance solution and the collection of liquid by the suction system were verified, which deposits the waste into a container. By using a pigment, the direction and replacement of the liquid were observed, establishing a constant flow without spills. The perfusion chamber was filled at a flow rate of 0.9 mL/min, while the suction system was set between 8 and 12 mL/min, ensuring that the liquid did not return.

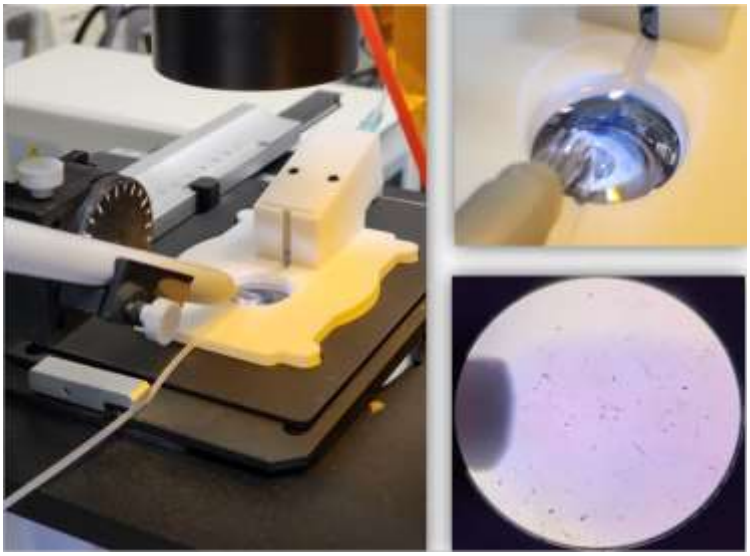


Figure 13. Tests of the Cellular Activity Recording Unit functionality in a real-world scenario.

To deliver the reagent, the micropipette capillaries were positioned at the center of the chamber, using the micromanipulator to adjust the angle and immerse the tips of the capillaries into the solution (Fig. 13). Through the microscope, the flow direction of the pigment and its continuous replacement were observed, keeping the area free of residues (Fig. 14). This ensures a continuous supply and allows an immediate cellular response upon contact with the reagent.

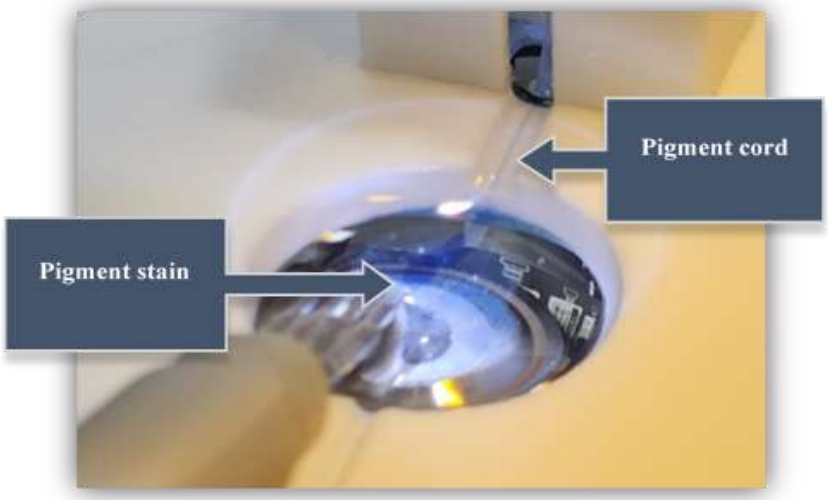


Figure 14. Top view of the perfusion chamber.

The tests confirmed proper reagent delivery to the cellular area and continuous washing. The results showed appropriate operating ranges for the efficient functioning of the systems, supporting future validation for in vitro fluorescence recordings (ex. Intracellular calcium with Fluo-4AM, or Reactive Oxygen Species by DCFH2-DA) by microperfusion in different adherent eukaryotic cell lines such as HEK-293, Neu2a and S. cerevisiae yeast through the use of activators or inhibitors of membrane proteins, such as purinergic receptors providing clean, immediate, precise and controlled cellular responses.

During the development of the design, several limitations were identified that affected the system's performance. First, the link corresponding to the Z-axis, responsible for supporting the X and Y axes, exceeds the load capacity of the motor assigned to that axis, preventing proper displacement. Second, the micromanipulator exhibited vibrations during movement due to the range of values sent by the potentiometers; although an error threshold was applied to reduce them, the system still requires a programming update. Finally, the suction system and the HMI screen showed a delay in transmitting values to the microcontroller, resulting in a slow response. To address these limitations, it is proposed to modify the Z-axis link design and integrate a more suitable motor, such as a Nema 17, capable of supporting loads between 1 and 5 kg; update the programming parameters of the micromanipulation system to improve movement stability and precision; and optimize the suction system programming to reduce response times. Additionally, potential improvements to the instruments are considered through the redesign of mechanical or aesthetic components, as well as the incorporation of new materials—such as aluminum, steel, or plastics—to develop

a more precise and robust model based on the current prototype.

The cellular activity recording unit is installed in a controlled area subject to environmental variables such as temperature, lighting, humidity, and vibrations. The latter represents a limitation, as the system does not include an anti-vibration table, a specialized piece of equipment that must be acquired separately for studies requiring higher precision.

Conclusions

The analysis of the results obtained allows us to conclude that the injection, micromanipulation, and suction systems meet the functional requirements for cellular studies, providing a continuous and adequate flow throughout the experiments. In the injection system, the solenoid valves ensure precise delivery of reagents by regulating the flow toward the perfusion chamber. The micromanipulator enables accurate positioning of the micropipette capillaries within the microscope's field of view, facilitating targeted reagent application. Likewise, the suction system efficiently removes the solution, directing it into a collection container. Altogether, these components form a Cellular Activity Recording Unit capable of supporting *in vitro* studies by enabling the observation of cellular fluorescence in response to reagent administration in microperfusion studies. The advantage of this integrated equipment is that it does not require sterilization; it only requires that its components such as syringes, micropipette, chamber, and tubing be kept clean and dry at the end of each recording.

Additionally, the instruments developed exhibit a compact design and allow intuitive user interaction through manual and software-based control. Their maintenance is cost-effective due to the use of accessible and low-cost materials, representing a substantially more economical alternative to commercial systems priced between $9,000 and $40,000 USD. Nevertheless, further testing is required to strengthen data reliability and enhance operational precision. These additional evaluations will help identify areas for improvement and maintenance needs, contributing to optimal long-term performance.

Finally, future work will focus on expanding the scope of the system by integrating improvements and adaptations to the prototypes and by conducting more advanced *in vitro* cellular studies. These developments will enable more complex operations and help ensure the project's sustainability and long-term scientific impact.

Funding

The authors received no specific funding for this work.

Acknowledgments

The authors gratefully acknowledge the Faculty of Professional Studies of the Zona Media of UASLP for providing the facilities, infrastructure, and equipment required for the development of this work.

References

[1] Chari S. Micro Electro Mechanical Systems (MEMS): Fabrication using DEMATEL method. Journal on Emerging Trends in Modeling and Manufacturing. Vol. 9, no. 2, pp. 35-44, 2023.

[2] Chircov C., Grumezescu A. Microelectromechanical Systems (MEMS) for Biomedical Applications. Micromachines. Vol. 13, no. 2, pp. 1-31, 2022.

[3] Chang B., Liu X., Bertram N., Han A. Flexible BioMEMS devices enabled by micromachining of plasma-polymerized

fluorocarbon. Micro and Nano Engineering. Vol. 19, no. 1, pp. 1-7, 2023.

[4] Caglayan Z., Demircan Y., Kulah H. A Prominent Cell Manipulation Technique in BioMEMS: Dielectrophoresis. Micromachines. Vol. 11, no. 11, pp. 1-36, 2020.

[5] Sha X., Sun H., Zhao Y., Li W., Li W. A review on microscopic visual servoing for micromanipulation systems: applications in micromanufacturing, biological injection and nanosensor assembly. Micromachines. Vol. 10, no. 12, 2019.

[6] Wang W., Liu X., Gelinas D., Ciruna B., Sun Y. A fully automated robotic system for microinjection of zebrafish embryos. PLOS One. Vol. 2, no. 9, pp. 1-8, 2007.

[7] Guo X., Zhao A., Zhang Y. Design and testing of a new microinjector with FBG force sensor for robot-assisted single cell microinjection. Measutement. Vol. 221, no. 1, 2023.

[8] Jonsson A., Toppi A., Dufva M. The FAST pump, a low-cost, easy to fabricate, SLA-3D-printed peristaltic pump for multi-channel systems in any lab. HardwareX. Vol. 8, 2020.

[9] Ching T., Vasudevan J., Tan H. Highly-Customizable 3D printed peristaltic pump kit. HardwareX. Vol. 10, 2021.

[10] Xiang J., Cai Z., Zhang Y., Wang W. A micro-cam actuated linear peristaltic pump for microfluidic applications. Sensors and Actuators A: Physical. Vol. 251, 2016.

[11] Abello J., Raghavan S., Yien Y., Stratman A. Peristaltic pumps adapted for laminar flow experiments enhance in vitro modeling of vascular cell behavior. Journal of Biological Chemistry. Vol. 298, no. 10, pp. 1-11, 2022.

[12] Alamsyah F. The kinematics analysis of a robotic arms manipulators cylindrical robot RPP type for FFF 3D printing using Scilab. IOP Conference Series Materials Science and Engineering. Vol. 494, pp. 1-9, 2019.

[13] Gasoto S., Schneider B., Setti J. Study of the pulse of peristaltic pumps for use in 3D extrusion bioprinting. ACS Omega. Vol. 7, no. 28, pp. 24091-24101, 2022.